THE PROTEIN SOCIETY

# High-resolution crystal structures reveal a mixture of conformers of the Gly61-Asp62 peptide bond in an oxidized flavodoxin from *Bacillus cereus*

**Ingvild Gudim,[1] Marie Lofstad,[1] Wouter van Beek,[2] and Hans-Petter Hersleth [1,3]***

[1]Department of Biosciences, Section for Biochemistry and Molecular Biology, Department of Biosciences should be before Section for Biochemistry and Molecular Biology, University of Oslo, Oslo, Norway

[2]Swiss-Norwegian Beam Lines, European Synchrotron Radiation Facility, Grenoble, France

[3]Department of Chemistry, Section for Chemical Life Sciences, University of Oslo, Oslo, Norway

Received 15 March 2018; Accepted 27 April 2018
DOI: 10.1002/pro.3436
Published online 3 May 2018 proteinscience.org

**Abstract: Flavodoxins (Flds) are small proteins that shuttle electrons in a range of reactions in microorganisms. Flds contain a redox-active cofactor, a flavin mononucleotide (FMN), and it is well established that when Flds are reduced by one electron, a peptide bond close to the FMN isoalloxazine ring flips to form a new hydrogen bond with the FMN N5H, stabilizing the one-electron reduced state. Here, we present high-resolution crystal structures of Flavodoxin 1 from *Bacillus cereus* in both the oxidized (ox) and one-electron reduced (semiquinone, sq) state. We observe a mixture of conformers in the oxidized state; a 50:50 distribution between the established oxidized conformation where the peptide bond is pointing away from the flavin, and a conformation where the peptide bond is pointing toward the flavin, approximating the conformation in the semiquinone state. We use single-crystal spectroscopy to demonstrate that the mixture of conformers is not caused by radiation damage to the crystal. This is the first time that such a mixture of conformers is reported in a wild-type Fld. We therefore carried out a survey of published Fld structures, which show that several proteins have a pronounced conformational flexibility of this peptide bond. The degree of flexibility seems to be modulated by the presence, or absence, of stabilizing interactions between the peptide bond carbonyl and its surrounding amino acids. We hypothesize that the degree of conformational flexibility will affect the Fld ox/sq redox potential.**

**Keywords: flavodoxin; X-ray crystallography; single-crystal spectroscopy; peptide flip; flavoprotein; redox protein**

## Introduction

Flavodoxins (Flds) are small electron transfer proteins that are involved in a variety of reactions in microorganisms. They participate, for example, in the photosynthetic reduction of $NADP^+$, in nitrogen fixation, and in the reductive activation of various enzymes, such as pyruvate formate-lyase, biotin synthase, ribonucleotide reductase, cytochrome P450 BioI, and bacterial nitric oxide synthase.[1–8] Furthermore, Flds have been shown to be essential in some pathogenic bacteria, for example *Helicobacter pylori* and *Streptococcus pneumoniae,* and are therefore a potential drug target.[9,10]

Structurally, the Flds have a three-layer αβα fold, consisting of a central five-stranded parallel

Additional Supporting Information may be found in the online version of this article.

Grant sponsor: The Research Council of Norway; Grant number: 231669; Grant sponsor: University of Oslo.

*Correspondence to: Hans-Petter Hersleth, Section for Biochemistry and Molecular Biology, Department of Biosciences, University of Oslo, P.O. Box 1066 Blindern, 0316 Oslo, Norway. E-mail: h.p.hersleth@ibv.uio.no

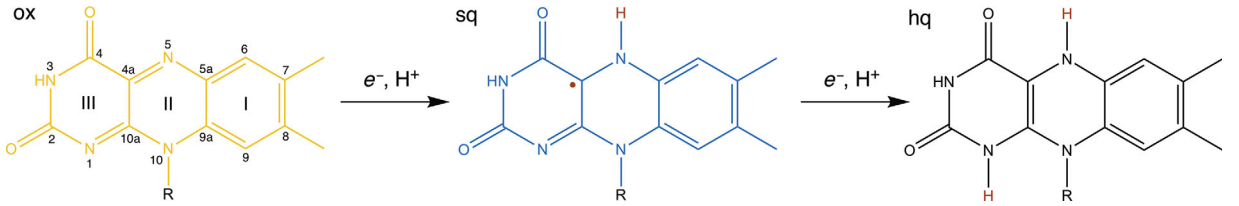


**Scheme 1.** Oxidation states of the FMN cofactor: oxidized (ox), semiquinone (sq) and hydroquinone (hq). The numbering of the flavin isoalloxazine ring is also shown.

β-sheet that is surrounded by two layers of α-helices. The Flds can furthermore be divided into two groups, short-chain and long-chain Flds, where the long-chain proteins have an additional 20-residue loop.[1] Moreover, all Flds contain a tightly bound flavin mononucleotide (FMN) as a redox cofactor. FMN can exist in three possible oxidation states (Scheme 1); oxidized FMN (ox), one-electron reduced FMNH• (semiquinone, sq), and two-electron, fully reduced $FMNH^-$ (hydroquinone, hq). Free FMN in solution has markedly different redox potentials than when associated with the protein. Flds stabilize the semiquinone state of the FMN cofactor and destabilize the hydroquinone state, resulting in sq/hq redox potentials that often are less than −400 mV. This protein-induced modification of the FMN redox couples contributes to the function of Flds as low potential electron carriers in the cell.[1,3,11–15]

The nature of the flavin–protein interactions, and how these contribute to the separation of the redox couples in the holoprotein as compared to free FMN, has been extensively studied in the last two decades. Electrostatic interactions, aromatic interactions, sulfur–flavin interactions, and hydrogen-bonding interactions have all been found to affect the flavin midpoint potential.[1,11,12] Additionally, a conformational change that occurs upon reduction of the flavin from the oxidized to the one-electron reduced semiquinone state has been found to be particularly important for the stabilization of the semiquinone state. A main chain carbonyl in the loop that binds the flavin isoalloxazine ring flips from a conformation where the carbonyl group is pointing away from the flavin ("O-down") to a conformation where it is pointing toward the flavin ("O-up") (Fig. 1).[16] The N5 atom on the flavin isoalloxazine ring is protonated in the sq state, but not in the ox state. The peptide flip, therefore, allows for the formation of a hydrogen bond between the carbonyl and the now protonated N5H, stabilizing the semiquinone state relative to the oxidized form.

In most short-chain Flds, this peptide flip involves a glycine residue that has been shown to be functionally important. Ludwig *et al*. replaced Gly57 by a series of other amino acids in the *Clostridium beijerinckii* Fld and examined the redox potentials and crystal structures of the various mutants.[11] The crystal structures showed that all the mutants examined underwent the O-down to O-up transition upon reduction, even if the mutation introduced considerable steric restraints. However, the ox/sq redox potentials of the mutants decreased relative to the wild-type protein, and a later follow-up study by Chang and Swenson demonstrated that the hydrogen bond interaction between the carbonyl and the flavin N5 atom correlates with the observed redox potentials for the ox/sq couple, that is, the wild-type glycine residue provides the strongest hydrogen-bond interaction.[11,13] Hence, it seems likely that the small size and structural flexibility of glycine is important for the modulation of the $E_{ox/sq}$ redox potential in short-chain Flds.[13]

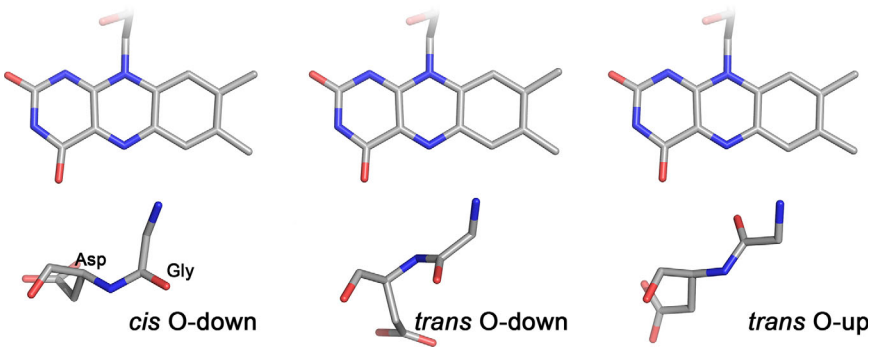


**Figure 1.** The three observed conformations of the Fld peptide backbone that interacts with the N5 atom on the flavin isoalloxazine ring as described by Ludwig *et al*.[11] Explanation of the nomenclature: if the Gly carbonyl O is pointing toward the FMN N5 atom it is called "up," and if it is pointing away it is called "down." The *cis*/*trans* refer to whether the Gly-Asp peptide bond is in a *trans* or *cis* conformation. The figure is made using the *C. beijerinckii* Fld structures with PDB IDs: *5nll* (*cis* O-down), *2fax* (*trans* O-down), and *2fox* (*trans* O-up).

**Table I.** *Data Collection and Refinement Statistics*

| | Fld1(ox) Crystal 1 | Fld1(sq) Crystal 2 | Fld1(ox) Crystal 3 |
|---|---|---|---|
| Data collection | | | |
| X-ray source | BM01A, ESRF | BM01A, ESRF | BM01A, ESRF |
| Wavelength (Å) | 0.698 | 0.698 | 0.700 |
| Space group | $P2_122_1$ | $P2_122_1$ | $P2_122_1$ |
| *a*, *b*, *c* (Å) | 38.9, 45.1, 82.4 | 38.9, 45.1, 82.0 | 38.8, 44.9, 81.4 |
| Rotation range per image (°)[a] | 0.55/1.5 | 0.6/1.5 | 0.4 |
| Total rotation range (°)[a] | 121/120 | 120/120 | 120 |
| Exposure time per image (s)[a] | 24/3 | 27/3 | 15 |
| Flux (ph/s) | $3.0 \times 10^{10}$ | $3.0 \times 10^{10}$ | $5.9 \times 10^{9}$ |
| Beam size ($\mu m^2$) | $260 \times 325$ | $260 \times 325$ | $240 \times 240$ |
| Crystal size ($\mu m^3$) | $250 \times 250 \times 50$ | $500 \times 300 \times 100$ | $100 \times 100 \times 40$ |
| Absorbed X-ray dose (MGy) | | | |
| Average dose | 0.50 | 0.47 | 0.22 |
| Average diffraction weighted dose | 0.30 | 0.28 | 0.10 |
| Mosaicity (°) | 0.47 | 0.73 | 0.31 |
| Resolution range (Å) | 35.20–1.27 (1.29–1.27) | 35.15–1.32 (1.34–1.32) | 39.29–1.40 (1.42–1.40) |
| Total no. of reflections | 201,713 | 190,562 | 104,466 |
| No. of unique reflections | 38,813 | 34,618 | 28,302 |
| $R_{meas}$ | 0.055 (0.085) | 0.051 (0.102) | 0.077 (0.524) |
| $R_{merge}$ | 0.050 (0.070) | 0.046 (0.090) | 0.067 (0.432) |
| Completeness (%) | 99.3 (90.8) | 99.8 (99.4) | 98.8 (99.7) |
| Multiplicity | 5.2 (3.6) | 5.5 (4.8) | 3.7 (3.0) |
| $<I/\sigma(I)>$ | 19.7 (9.8) | 23.2 (13.6) | 15.6 (1.4) |
| $CC_{1/2}$ | 0.998 (0.992) | 0.998 (0.989) | 0.997 (0.671) |
| Refinement statistics | | | |
| $R_{work}/R_{free}$ | 15.1/17.1 | 10.5/12.6 | 17.8/20.5 |
| Mean protein/solvent isotropic *B* factor ($Å^2$) | 8.0/19.2 | 8.1/20.8 | 12.6/24.3 |
| Total modeled atoms (non-H) | 1617 | 1640 | 1527 |
| Protein residues | 147 | 147 | 147 |
| Ligand atoms (1 FMN, 1 sulfate, 1 glucose) | 48 | 48 | 48 |
| Added waters | 217 | 182 | 173 |
| Solvent content (%) | 45.3 | 44.9 | 44.1 |
| Matthews coefficient | 2.25 | 2.23 | 2.20 |
| Ramachandran plot: most favored/allowed | 98.6/1.4 | 99.3/0.7 | 99.3/0.7 |
| RMSD bond lengths (Å) | 0.007 | 0.009 | 0.017 |
| RMSD bond angles (°) | 1.27 | 1.40 | 1.78 |
| Estimated overall coordinate error based on maximum likelihood (Å) | 0.080 | 0.070 | 0.140 |
| PDB ID | *6fsg* | *6fsi* | *6ft1* |

[a] The value after the backslash is for the low resolution data set collected to 2.2 Å.
The values in parenthesis are for the highest resolution shell.

Although considerable research has been devoted to the stabilization of the flavin semiquinone by this peptide flip, rather less attention has been paid to another finding by Ludwig *et al*., namely that one of the mutant Flds exhibits a flip already in the oxidized state. Ludwig *et al*. observed that the Gly57-Asp58 peptide carbonyl in the wild-type *C. beijerinckii* crystal structure formed a hydrogen bond with Asn137 in the neighboring protein molecule. They removed this interaction by constructing an Asn137Ala mutant, and in the mutant crystal structure they observed a mixture of three conformers of the Gly57-Asp58 peptide bond. They estimated the distribution of the different conformers to be 50% in the *cis* O-down conformation, 20% in the *trans* O-down conformation, and 30% in the *trans* O-up conformation (Fig. 1).[11] The O-up conformer had only previously been seen in the semiquinone form, but Ludwig *et al*. proposed that this mixture of conformers is likely representative for the solution behavior of the wild-type Fld and that the conformational energies of the three conformers in *C. beijerinckii* are very similar. If these results could be confirmed for a wild-type protein and preferably also in a different organism, it would provide strong evidence that the well-known peptide flip in reduced Flds is not strictly associated with the flavin oxidation state, but that it is also dependent on the protein amino acid sequence and the stabilization of the possible conformers in the protein.

Here, we present three high-resolution crystal structures of a Fld from *Bacillus cereus* where we see a mixture of O-up and O-down conformers of the Gly61-Asp62 peptide bond in the oxidized state. The oxidized *trans* O-up conformer differs slightly from the strictly *trans* O-up conformation observed in the semiquinone crystal structure of the same protein, which is

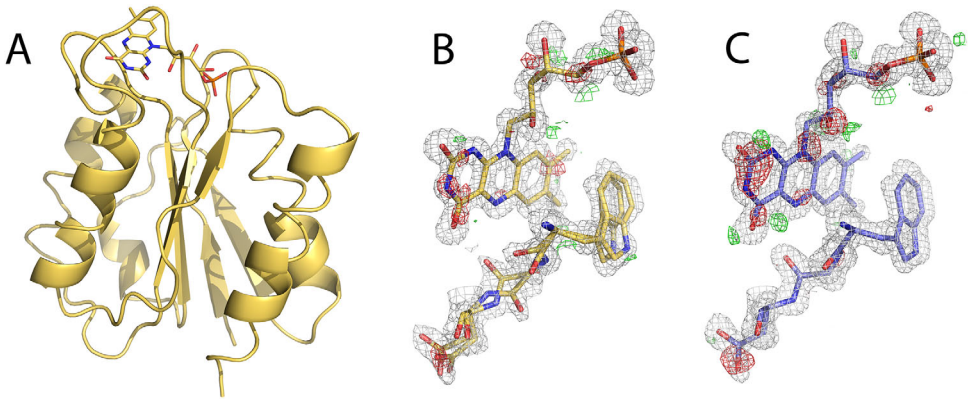


**Figure 2.** A: Crystal structure of Fld1 from *B. cereus*. B: The Trp60-Gly-Asp62 turn in oxidized Fld1 (Crystal 1), showing clear electron density for a mixture of conformers around the Gly-Asp peptide bond. C: The Trp60-Gly-Asp62 turn in the one-electron reduced, sq Fld1, where the electron density indicates only one conformation of the Gly peptide bond. The $2F_o - F_c$ maps in (B,C) are contoured at $1\sigma$, and the $F_o - F_c$ maps are contoured at $\pm 3\sigma$.

also presented here. We have used single-crystal spectroscopy to demonstrate that the mixture of conformers that we observe is not a result of radiation damage. To our knowledge, this is the first time a distribution of conformations of the glycine peptide bond has been confirmed for a wild-type Fld *in crystallo*.

## Results

### *Structure of Flavodoxin 1*

The crystal structure of the oxidized Flavodoxin 1 (Fld1) from *B. cereus* has been refined to a resolution of 1.27 Å (see Crystal 1 in Table I). The structure, shown in Figure 2(A), is typical of that of a short-chain Fld, with a five-stranded β-sheet surrounded by α-helices. There is also clear electron density for an FMN molecule [Fig. 2(B)]. Tyr96 forms a stacking interaction with the flavin ring on the *si* face, whereas the residues Trp60-Gly-Asp-Gly63 form a turn that interacts with the N5 edge of the flavin isoalloxazine ring. Gly61, which is located just opposite the N5 isoalloxazine atom, cannot be adequately modeled in the *trans* O-down conformation, the expected conformation for an oxidized Fld. Rather, the electron density map suggests a mixture of conformers, with both *trans* O-down and *trans* O-up conformers of the Gly61-Asp62 peptide bond [Fig. 2(B)]. The peptide bond was successfully modeled by introducing two conformations of the Trp60-Gly-Asp62 motif, resulting in both the O-up and O-down conformers of Gly61 to refine to occupancies of 0.5 in phenix.refine.[17] The omit maps of the respective O-down and O-up conformers clearly support that both conformers are present (Fig. 3).

Data from a second crystal of the oxidized Fld (Crystal 3, Table I) was solved and refined to 1.40 Å, and also showed a mixture of the O-up and O-down conformers (Supporting Information Fig. S3). Here, the O-up and O-down conformers of Gly61 refine to an occupancy of 0.4 and 0.6, respectively.

We have also solved the structure of the *B. cereus* Flavodoxin 1 in the semiquinone state (Crystal 2 in Table I). As expected, the Gly61-Asp62 bond is strictly in a *trans* O-up conformation [Fig. 2(C)]. Even so, the carbonyl is shifted slightly closer to the isoalloxazine ring compared to the *trans* O-up conformer in the oxidized structures. In the semiquinone structure, the distance between the *trans* O-up carbonyl and the N5 atom on the isoalloxazine ring is 2.99 Å, equivalent to a medium-strength hydrogen bond, whereas in the oxidized structure, the N5–O61 distance (for the *trans O*-up conformer) is 3.19/3.16 Å (for Crystal 1/Crystal 3), a slightly weaker hydrogen-bond interaction.

### *Single-crystal spectroscopy*

All protein crystals are damaged by the high energy X-rays that the crystals are exposed to during data collection, but redox cofactors are especially prone to radiation damage and radiation-induced reduction.[18,19] We have monitored the oxidation state of oxidized Fld1

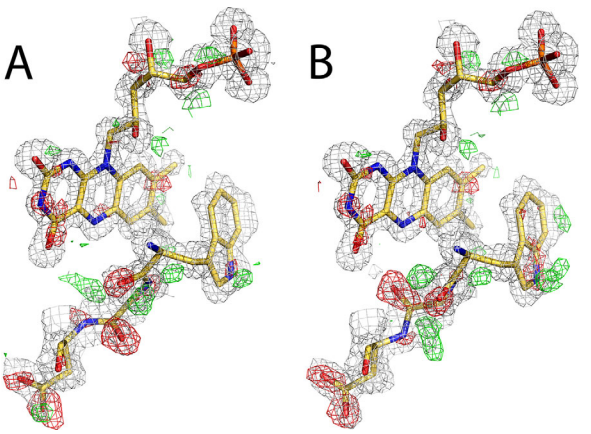


**Figure 3.** Omit maps of the O-up (Panel A) and O-down (Panel B) conformers in crystal 1. The $2F_o - F_c$ maps are contoured at $1\sigma$, and the $F_o - F_c$ maps are contoured at $\pm 3\sigma$.

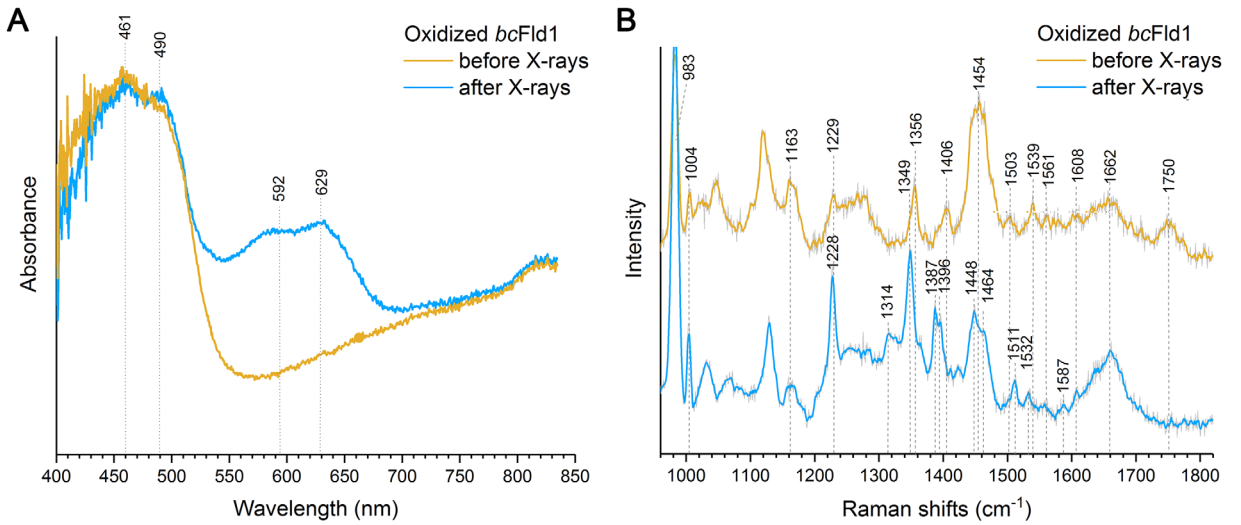


**Figure 4.** Single-crystal UV–vis (Panel A) and Raman (Panel B) spectra of oxidized Fld1 before (yellow line) and after (blue line) X-ray data collection. The UV–vis measurements are recorded on Crystal 1 and Raman measurements are recorded on Crystal 3 (Table I).

crystals by recording single-crystal UV–vis (Crystal 3 in Table I) and Raman (Crystal 1 in Table I) spectra before and after X-ray exposure. The spectra, shown in Figure 4, confirm that the crystals are in the fully oxidized state before data collection, and that the flavin cofactor has been partly reduced by the X-rays at the end of the data collection, as has previously been observed for the Fld-like protein NrdI from *B. cereus*.[20] The optical single-crystal spectrum recorded before exposure to X-rays shows features that are characteristic for an oxidized Fld, with peaks at 461 and 490 nm, while the spectrum collected after crystal X-ray exposure shows a peak around 600 nm, which is typical for the one-electron reduced semiquinone state [Fig. 4(A)]. Similarly, the single-crystal Raman spectrum collected before X-ray exposure [Fig. 4(B)] corresponds well with the single-crystal Raman spectra of the oxidized Fld-like protein NrdI.[20] In particular, both the presence of the modes at 1356 $cm^{-1}$ [assigned for NrdI as $\nu$(ring I,II,III), $\delta(NH_3$-H)] and at 1406 $cm^{-1}$ [assigned for NrdI as $\nu$(ring I,II), methyl deformation], as well as the absence of modes at 1349 $cm^{-1}$ [assigned for NrdI as $\delta$(N5-H), $\delta$(N3-H), $\nu$(ring I,II,II)] and at 1396 $cm^{-1}$ [assigned for NrdI as $\nu$(ring I), $\nu$(N5-C4a), $\nu$(C10a-N1)] are characteristic of oxidized Fld, compared to the semiquinone single-crystal Raman spectra.[20] Likewise, the spectral changes observed after the Fld1 crystal has been exposed to X-rays [Fig. 4(B)] also resemble the spectral changes of X-ray exposed NrdI crystals. The increasing modes at 1349 and 1387/1396 $cm^{-1}$ and the diminishing modes at 1356 and 1406 $cm^{-1}$, as well as the shifts of modes 1503 and 1539 to 1511 and 1532 $cm^{-1}$, respectively, are characteristic of the change from the oxidized to the semiquinone state that is reported for NrdI crystals.[20]

Structurally, the oxidized and semiquinone Flavodoxin 1 structures also show another sign of radiation-induced reduction: a slight butterfly bend of the isoalloxazine ring along the N5–N10 axis (Fig. 5). This is similar (although less pronounced) to what has been observed for radiation-influenced structures of NrdI, where QM/MM (quantum mechanics/molecular mechanics) calculations showed that this bend is a result of a one-electron reduction of the FMN-group.[20]

## Discussion

### *A mixture of up- and down-conformers is observed for* B. cereus *Flavodoxin 1*

It is well established that a peptide bond carbonyl forms a hydrogen bond with the protonated N5 atom on the isoalloxazine ring when a Fld is in the

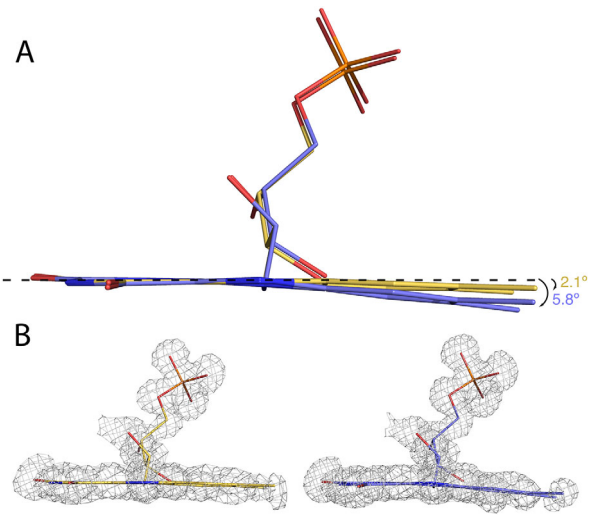


**Figure 5.** Flavin butterfly bend. A: The bending of the plane in the oxidized (yellow) and semiquinone (blue) structures, compared to a planar model indicated by a dashed line. B: The electron density of the flavin cofactor in the oxidized (yellow) and semiquinone (blue) structures.

one-electron reduced semiquinone state, locking the peptide bond in an "O-up"-conformation that stabilizes the semiquinone state. However, Ludwig *et al*. proposed that oxidized Flds might have a mixture of up- and down-conformers of the Gly57-Asp58 peptide bond in solution, implying that the peptide flip is not strictly dependent on the protein oxidation state. Rather, if the conformational energies of the O-up and O-down conformers are similar enough, there will be a mixture of conformers even in the oxidized state. This finding seems to have gone largely unnoticed, and, to our knowledge, has not been conclusively confirmed. The mixture of conformers that we observe in the oxidized *B. cereus* Fld crystal structure underpins the proposition set forward by Ludwig *et al*.

### *A structural survey indicates that conformational flexibility of the glycine peptide bond is common*

Interestingly, a closer look at the published Fld structures in the Protein Data Bank reveals that there are actually more Fld structures where the peptide bond is flipped, fully or partly, to the O-up conformation already in the oxidized state. We have evaluated the interactions between the peptide bond carbonyl that flips and its surrounding amino acids, and compared these structures to Fld structures where the peptide bond only flips upon reduction. Indeed, it does seem like the differential conformational energies play an essential role in determining whether or not the peptide bond is flipped already in the oxidized state. Figure 6 shows an overview of different peptide conformations in the oxidized and one-electron reduced state of Flds and Fld-like proteins from *Eschericia coli* (*ec*), *Helicobacter pylori* (*hp*), *Azotobacter vinelandii* (*av*), *Nostoc sp* (*ns*), *Synechococcus elongatus* (*se*), *Clostridium beijerinckii* (*cb*), *Lactobacillus reuteri* (*lr*), *Streptococcus pneumoniae* (*sp*), *Desulfovibrio desulfuricans* (*dd*), *Desulfovibrio gigas* (*dg*), *Desulfovibrio vulgaris* (*dv*), *Bacillus anthracis* (*ba*), *Bacillus cereus* (*bc*), and *Bacillus subtilis* (*bs*). First, several structures have a mixture of conformers. In the oxidized *bc*Fld1 structure [Fig. 6(A)], the structure presented in this article, the peptide-bond carbonyl is close (2.5 Å) to the carboxyl group of Asp64 in the O-down state, while in the O-up state it is close (3.2 Å) to the isoalloxazine N5 atom. Neither state is favorable for hydrogen bonding, which explains the approximately 50:50 distribution observed between the O-up and O-down conformers in the *bc*Fld1 oxidized state. Similarly, in the aforementioned structures of oxidized *cb*Fld [Fig. 6(B)] by Ludwig *et al*.,[11] the O-down state is stabilized by an intermolecular hydrogen bond to Asn137 in the crystal. However, by mutating Asn137 to Ala, the hydrogen bond is disrupted and a mixture of O-up and O-down is observed [Fig. 6(C)], suggesting that there is a mixture of conformations in solution for the oxidized wild-type protein too. Furthermore, both the *av*Fld structure and the NMR-structure of *ec*Fld1 indicate a mixture of O-up and O-down conformers [Fig. 6(I,M)]. The *av*Fld structure has poor electron density for Gly58. We see no clear stabilization of the modeled O-down conformer, and we expect that there is in fact a mixture of conformers in the crystal. The different structures in the *ec*Fld1 ensemble NMR-structure show a mixture of O-up and O-down conformers, and it does not seem to be a clear stabilization of the O-down conformation. Second, several structures, namely *dd*Fld, *sp*Fld, *hp*Fld, *se*Fld, *bc*NrdI, and *bs*NrdI, have an intramolecular hydrogen bond stabilizing the O-down conformation [Fig. 6(D,H,K,L,N,O)], hence there is no flip to the O-up conformation in the oxidized states of these proteins. In contrast to these structures where the O-down conformation is stabilized, the oxidized *dg*Fld structure [Fig. 6(F)] has a complete flip/O-up conformation, where the carbonyl group is stabilized by a hydrogen bond to a water molecule. The authors suggested that the O-up peptide conformation might be due to radiation damage causing the flavin cofactor to be reduced, but a closer look on the possible hydrogen-bonding interactions provides, in our opinion, a better explanation. However, it is difficult to rationalize the observed conformation for some of the structures, for example the *dv*Fld structure, which is in the O-down conformation, but has both stabilizing as well as destabilizing interactions [Fig. 6(E)]. Also, *se*Fld is stabilized by a hydrogen bond to a water molecule in the crystal, making it difficult to predict which conformer(s) will be present in solution [Fig. 6(L)]. Third, several of the long-chain Flds have other residues than Gly in the flipping position (see sequence alignment, Supporting Information Fig. S1). Therefore, even though there is no clear stabilization nor destabilization of the peptide bond carbonyl in these Flds, it might be that it is merely the decreased flexibility of these residues that leads to the strictly O-down conformation in the oxidized state, as seen for *ns*Fld [Fig. 6(J)]. This notion is supported by the mutational study carried out by Ludwig *et al*., who found that mutating glycine to bulkier, less flexible residues increases the conformational energy of the O-up conformer in the oxidized state.[11] To sum up, our structural survey indicates that the interactions of the glycine peptide bond carbonyl with the surrounding amino acids can provide enough stabilization for the peptide bond to flip to an O-up conformation already in the oxidized state.

NMR studies on other Flds also indicate that there is a mixture of conformers in solution. Work on the Flds MioC,[21] FldA,[22] and YqcA[22] from *E. coli* by Jin and coworkers show that conformational exchanges are especially pronounced in the apo-form

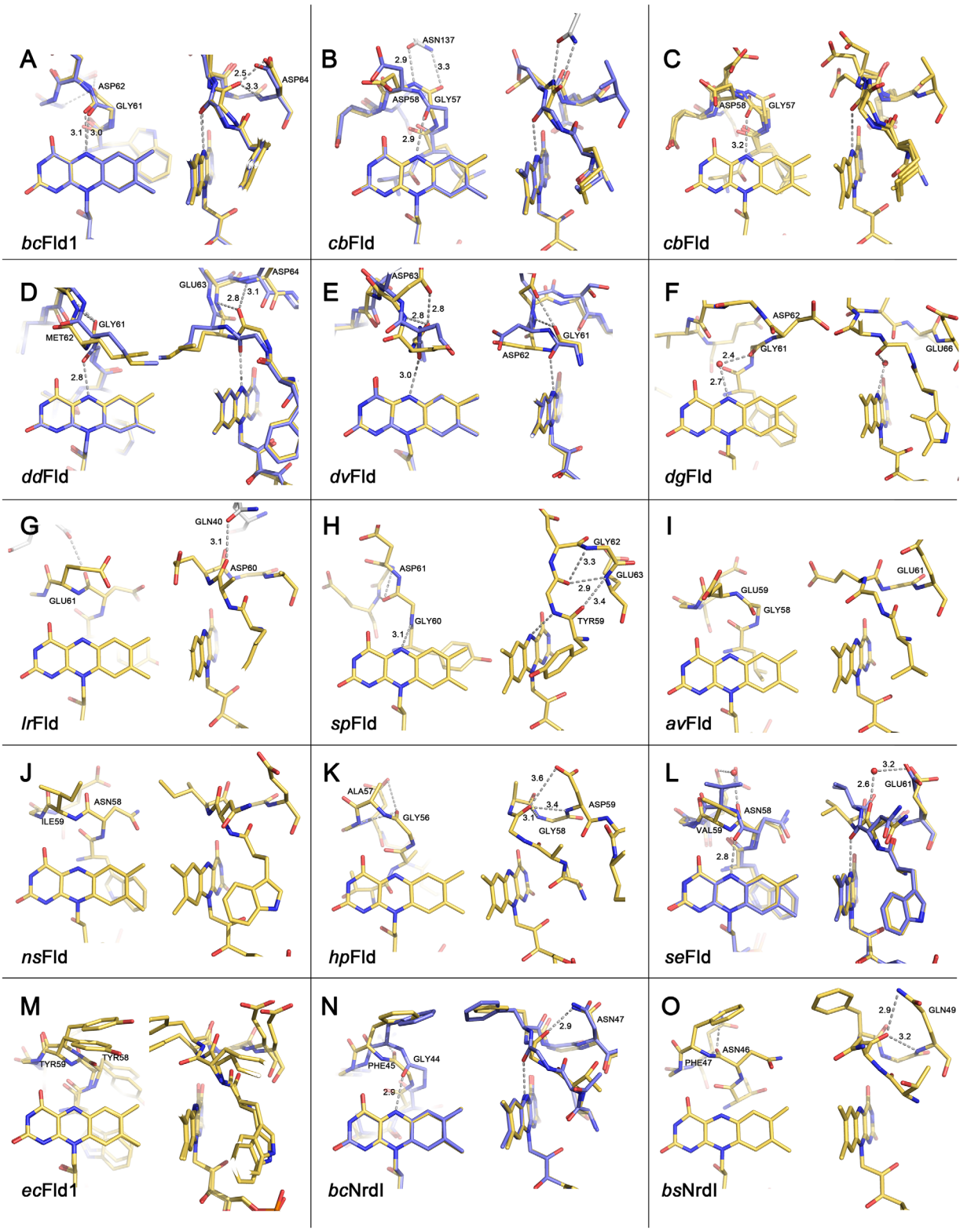


**Figure 6.** Comparison of the flavin isoalloxazine binding site of different deposited Fld and NrdI structures. Key residues involved in the potential peptide flip are shown. The oxidized structures are colored with yellow carbon atoms, and the semiquinone structures with light blue carbon atoms. PDB IDs are listed in the Material and methods section.

of the proteins, probably to facilitate FMN-binding. However, conformational exchanges are still observed in the corresponding holo-proteins, but now mostly in the isoalloxazine-binding loop.[21,22] Jin and coworkers suggest that the observed conformational sampling in the oxidized state could prime the protein for the structural changes that occur upon reduction to the semiquinone oxidation state, where the peptide bond is

locked in an O-up conformation. This notion of conformational sampling is supported by our observation that the distance between the carbonyl oxygen and the isoalloxazine N5 atom is different in the semiquinone crystal structure and in the oxidized O-up conformer. Taken together, the NMR and the X-ray crystallography data suggest that there is indeed conformational flexibility in the isoalloxazine-binding loop and that the energetic barrier between the different conformations of the peptide bond is small in some organisms. Studies by Swenson and coworkers have shown that the energy of the semiquinone formation is affected if the conformational energy of the peptide turn that binds the isoalloxazine ring is altered.[11,12,14] Further studies should compare the ox/sq redox potentials of the wild-type Flds presented in our structural overview, to see whether having several conformations in the oxidized state indeed lowers the energy barrier for semiquinone formation.

### *The Fld crystals are experiencing radiation damage, but this is not causing the peptide bond flip*

It is well known that radiation damage can cause reduction of redox-active sites in proteins, however, we do not believe that the observed mixture of conformations is due to X-ray reduction of the protein crystal. A previous study from our group on the effect of X-rays on NrdI, a Fld-like protein, shows that the flavin cofactor itself is reduced during data collection, and as a consequence the isoalloxazine ring changes geometry to a butterfly bend, but that the protein main chain, including the Gly45 carbonyl, is unperturbed [Fig. 6(N)].[20] The Fld structures presented here experience a similar, but smaller change of 2.1° (oxidized) and 5.8° (semiquinone) bending of the flavin plane, which still indicates a similar radiation effect as observed in NrdI. The NrdI study also showed that the radiation-reduced structure was only reduced by one electron and that the accompanying protonation of the N5 isoalloxazine atom did not occur. Therefore, even if the protein crystal experiences radiation-induced reduction, the peptide bond carbonyl does not flip because of the reduced cofactor, as there is no proton to form a hydrogen bond to. Furthermore, the single-crystal UV–vis and Raman spectra collected before and after data collection closely resemble the spectra observed for the NrdI crystals, indicating a similar radiation effect. In particular, the Raman bands at 1356, 1406, 1503, and 1539 $cm^{-1}$, as described in the Results section, more or less fully disappear, while new features appear at 1349, 1387/1396, 1511, and 1532 $cm^{-1}$. This is more consistent with a complete change of properties, such as a bend of the isoalloxazine ring, rather than a conformational change where approximately 50% of the proteins are in the original state and 50% are in a new O-up conformation. Finally, the electron density omit maps clearly support a 50:50 mixture of the O-down and O-up conformers. Therefore, we believe that the mixture of conformers that we see is representative for the solution behavior of *B. cereus* Fld1, and not radiation-induced behavior.

## Conclusions

Oxidized Flds have been suggested to have a mixture of O-up and O-down peptide conformations in the isoalloxazine-binding loop in solution, and this has now been confirmed *in crystallo* for a wild-type Fld. This mixture of conformers seems to be a relatively common feature; still it has been largely unnoticed or believed to be a result of radiation damage. The extent of the flip in the oxidized state depends on the conformational energies of the different conformers. In particular, the presence or absence of a hydrogen bond between the glycine peptide bond carbonyl and its surrounding amino acids that can stabilize the O-down conformation seem to be essential. This interaction is, most likely, important in tuning the redox properties of the Flds, and further studies should investigate the effect of the stabilization of the O-down confirmation on the ox/sq redox potential in wild-type Flds from different organisms.

## Material and Methods

### *Cloning, expression, and purification*

Genomic DNA was isolated from *B. cereus* ATCC 14579 using the DNEasy kit (Qiagen). The gene sequence encoding the Bc1376 Fld (Fld1) was then amplified by PCR, using gene-specific forward (GGAATTCCATATGAGTAAGTTAGTAATGATTTTTGC) and reverse (GCCGGATCCTTAAGAAAGGTGTTTTACAAATTCAGC) primers. The PCR product and the pET22b (+) expression vector (Novagen) were cut with FastDigest *NdeI* and *BamHI* restriction enzymes (Fermentas) and mixed for ligation. The ligation mixture was transformed into *E. coli* XL10-Gold Ultracompetent cells (Stratagene), from which enough plasmids were prepped to enable successful transformation of *E. coli* BL21 Gold (DE3) Competent cells (Novagen). Protein expression and purification of Fld1 was carried out in a similar fashion as previously described for the Fld-like protein NrdI.[20] Minor modifications from this protocol include the composition of the lysis buffer, which here contained 50 m*M* Tris-Cl buffer pH 7.5, 100 m*M* NaCl, 10 m*M* EDTA, 5% glycerol; the salt gradient in the anion exchange step, which was increased linearly from 200 to 500 m*M* KCl; and that the gel filtration step was carried out on a Superdex 75 10/300 GL gel filtration column (GE Healthcare) preequilibrated in gel filtration buffer (50 m*M* Tris-Cl buffer pH 7.5, 100 m*M* NaCl, 5% glycerol). This purification protocol gave a final yield of ~5 mg pure Fld1 per liter of culture.

The Fld1 concentration was estimated using a molar extinction coefficient of 10 $mM^{-1}$ $cm^{-1}$ at 450 nm.[4] The purity of the protein was confirmed with SDS-PAGE (sodium dodecyl sulfate-polyacrylamide gel electrophoresis).

### Crystallization

Crystallization screening was performed using the commercial crystallization screens JCSG+ (Molecular Dimensions) and Index (Hampton Research). Manual optimization of the JCSG+ F2 condition resulted in thick (100–500 μm) Fld1 crystals. The reservoir solution (600 μL) consisted of 3.6*M* ammonium sulfate and 0.1*M* citric acid pH 4 (final pH 5). The protein (20 mg $mL^{-1}$) and reservoir solution were mixed in a 1:1 ratio in a 4 μL drop, and set up as a sitting drop. The crystals were cryoprotected for 30 s in a cryo-solution containing 70% crystallization reservoir solution and 30% (wt/vol) glucose, before being flash-frozen in liquid nitrogen.

### Data collection and processing

X-ray data were collected at the Swiss-Norwegian Beam Line (SNBL) BM01A at the ESRF in Grenoble, France, at 100 K on a MAR345 image plate detector (Crystals 1 and 2) and a Dectris Pilatus 2M detector (Crystal 3). For Crystals 1 and 2 both a high- and a low-resolution dataset were collected. The diffraction data sets were integrated individually with iMosflm[23] and scaled and merged with Aimless.[24] The high- and low-resolution passes for Crystals 1 and 2 were merged together with Aimless. The protein structure was solved with molecular replacement using Phaser[25] with a Fld from *Desulfovibrio vulgaris* (PDB ID: *1wsb*)[26] that has 33% sequence identity as a search model. Several cycles of refinement were carried out using first Refmac5[27] and subsequently phenix.refine[17] in the Phenix suite.[28] For Crystals 1 and 2, the non-H atoms were made anisotropic, and hydrogen atoms included using a riding model, except for the hydroxyl hydrogen of serine, threonine, and tyrosine, as well as the imidazole hydrogen of histidines, which were not included. The Crystal 3 structure was refined isotropically without addition of hydrogen atoms. The standard Phenix restraints for the FMN group were loosened, and the isoalloxazine ring was made free to bend along the N5–N10 axis (butterfly bend). Model validation was performed using MolProbity.[29] Visualization and model building of the protein molecules were done in Coot.[30] Illustrations of the proteins were prepared with PyMOL.[31] The angle of the butterfly bend of the isoalloxazine ring was calculated with the psico module in PyMOL by calculating the angle between the two planes defined by the atoms N5, C4A, C4, N3, C2, C10, N10 and N5, C5A, C3, C47, C8, C9, C9A, N10 (Scheme 1). The absorbed X-ray doses were calculated with the program Raddose-3D[32,33] using the parameters listed in Table I. The beam size at the SNBL was defined with an X-ray Mini FDI Camera (Photonic Science). The photon flux was measured with a Canberra photodiode, type 300–500CB, calibrated for responsivity. Flux densities were calculated from the size and flux measurements and transformed to dose.

### Verification of the oxidation state of the flavin cofactor

The single-crystal Raman and UV–vis measurements were done at the SNBL at the ESRF, following an already published method.[20] Spectra of the oxidized Fld crystals were recorded before and after exposure to X-rays. UV–vis measurements were performed on Crystal 3 with a microspectrophotometer, model XSPECTRA (4DX System AB), equipped with a halogen lamp and an Oriel spectrometer with an Andor CCD camera (Andor Technology). A Renishaw inVia Raman microscope equipped with a 785 nm near-IR laser was utilized in backscattering mode for the Raman measurements on Crystal 1. The Raman spectra were baseline corrected to remove contributions from fluorescence and smoothed in Origin 9.1 (OriginLab Corp.). The original data before smoothing is shown in gray in Figure 4(B).

### Bioinformatic analysis

To compare the *B. cereus* Fld1 structure to other Fld structures, we searched the PDB database for the molecule name Fld, and selected all the structures that also contained an FMN group (i.e., holoprotein structures). This resulted in 76 deposited structures from 14 organisms with some organisms containing more than one Fld. Additionally, 11 structures of the Fld-like protein NrdI from a total of five organisms were found. The *B. cereus* Fld1 structure was used to perform a DALI search (DaliLite v. 3)[34] in the PDB-database for similar structures, and to perform multiple structural alignments. A Fld structure from each of the Flds and NrdIs described above were selected for the alignments. The structural sequence alignment from the DALI search is shown in Supporting Information Figure S1. A few sequences that differed to a large extent from the *B. cereus* Fld1 sequence were omitted for simplicity. The sequences are clustered into short-chain Flds, long-chain Flds, and NrdI proteins, based on the phylogenetic tree analysis with Blosum62 in Jalview[35] (Supporting Information Fig. S2). The coloring is done according to Clustal X, combined with color intensity adjusted to conservation by the AMAS method.[36] The secondary structure assignments shown in Supporting Information Figure S1 are performed with DSSP by the DALI server on the *B. cereus* Fld1 structure.[34] The structural alignment and phylogenetic analysis are based upon the following deposited structures in

the PDB-database (organism, abbreviation and PDB-ID listed for each): Flds; *Escherichia coli* (*ec*) *2mok* and *2mt9*, *Helicobacter pylori* (*hp*) *1fue*, *Azotobacter vinelandii* (*av*) *5k9b*, *Nostoc sp* (*ns*) *1flv*, *Synechococcus elongatus* (*se*) 1ofv, *Clostridium beijerinckii* (*cb*) *5nll*, *Lactobacillus reuteri* (*lr*) 5veg, *Streptococcus pneumoniae* (*sp*) *5lji*, *Desulfovibrio desulfuricans* (*dd*) 3kap, *Desulfovibrio gigas* (*dg*) *4heq*, *Desulfovibrio vulgaris* (*dv*) *3fx2*, NrdIs: *Bacillus anthracis* (*ba*) *2xod*, *Bacillus cereus* (*bc*) *2x2o*, *Bacillus subtilis* (*bs*) *1rlj*. For structural comparison of the flavin site and the surrounding residues of the Flds from different organisms (Fig. 4), the structures listed above have been used, in addition to the following semiquinone structures of *bc*Fld1, *cb*Fld *2fox*, *dd*Fld *3kaq*, *dv*Fld *4fx2*, *se*Fld *1czl*, *bc*NrdI *2x2p*, and the *cb*Fld *2fdx* mutant N137A. Figures were generated with PyMOL.[31]


## Acknowledgments

Authors thank Dr. B. Dalhus for access to crystallisation screening at the Regional Core Facility for Structural Biology and Bioinformatics at the South-Eastern Norway Regional Health Authority (grant HSØ 2015095). They also gratefully acknowledge the Swiss–Norwegian Beam Lines (SNBL) at the ESRF for providing beam time and access to online UV–vis and Raman spectroscopy and for excellent technical assistance. Authors declare no conflict of interest. X-ray coordinates and structure factors have been deposited in the PDB-database (PDB IDs: 6fsg, 6fsi, 6ft1).


## References


1. Sancho J (2006) Flavodoxins: sequence, folding, binding, function and beyond. Cell Mol Life Sci 63:855–864.
2. Nordlund P, Reichard P (2006) Ribonucleotide reductases. Annu Rev Biochem 75:681–706.
3. Mayhew SG, O'Connell DP, O'Farrell PA, Yalloway GN, Geoghegan SM (1996) Regulation of the redox potentials of flavodoxins: modification of the flavin binding site. Biochem Soc Trans 24:122–127.
4. Wang Z-Q, Lawson RJ, Buddha MR, Wei C-C, Crane BR, Munro AW, Stuehr DJ (2007) Bacterial flavodoxins support nitric oxide production by *Bacillus subtilis* nitric-oxide synthase. J Biol Chem 282:2196–2202.
5. Lawson RJ, von Wachenfeldt C, Haq I, Perkins J, Munro AW (2004) Expression and characterization of the two flavodoxin proteins of *Bacillus subtilis*, YkuN and YkuP: biophysical properties and interactions with cytochrome P450 BioI. Biochemistry 43:12390–12409.
6. Birch OM, Fuhrmann M, Shaw NM (1995) Biotin synthase from *Escherichia coli*, an investigation of the low molecular weight and protein components required for activity in vitro. J Biol Chem 270:19158–19165.
7. Ifuku O, Koga N, Haze S-I, Kishimoto J, Wachi Y (1994) Flavodoxin is required for conversion of dethiobiotin to biotin in *Escherichia coli*. Eur J Biochem 224: 173–178.
8. Blaschkowski HP, Knappe J, Ludwig-Festl M, Neuer G (1982) Routes of flavodoxin and ferredoxin reduction in *Escherichia coli*. Eur J Biochem 123:563–569.
9. Freigang J, Diederichs K, Schäfer KP, Welte W, Paul R (2002) Crystal structure of oxidized flavodoxin, an essential protein in *Helicobacter pylori*. Protein Sci 11: 253–261.
10. Rodríguez-Cárdenas Á, Rojas AL, Conde-Giménez M, Velázquez-Campoy A, Hurtado-Guerrero R, Sancho J (2016) *Streptococcus pneumoniae* TIGR4 flavodoxin: structural and biophysical characterization of a novel drug target. PLoS One 11:e0161020.
11. Ludwig ML, Pattridge KA, Metzger AL, Dixon MM, Eren M, Feng Y, Swenson RP (1997) Control of oxidation–reduction potentials in flavodoxin from *Clostridium beijerinckii*: the role of conformation changes. Biochemistry 36:1259–1280.
12. Kasim M, Swenson RP (2000) Conformational energetics of a reverse turn in the *Clostridium beijerinckii* flavodoxin is directly coupled to the modulation of its oxidation–reduction potentials. Biochemistry 39:15322–15332.
13. Chang F-C, Swenson RP (1999) The midpoint potentials for the oxidized–semiquinone couple for Gly57 mutants of the *Clostridium beijerinckii* flavodoxin correlate with changes in the hydrogen-bonding interaction with the proton on N(5) of the reduced flavin mononucleotide cofactor as measured by NMR chemical shift temperature dependencies. Biochemistry 38:7168–7176.
14. Kasim M, Swenson RP (2001) Alanine-scanning of the 50's loop in the *Clostridium beijerinckii* flavodoxin: evaluation of additivity and the importance of interactions provided by the main chain in the modulation of the oxidation–reduction potentials. Biochemistry 40: 13548–13555.
15. O'Farrell PA, Walsh MA, McCarthy AA, Higgins TM, Voordouw G, Mayhew SG (1998) Modulation of the redox potentials of FMN in *Desulfovibrio vulgaris* flavodoxin: thermodynamic properties and crystal structures of glycine-61 mutants. Biochemistry 37:8405–8416.
16. Smith WW, Burnett RM, Darling GD, Ludwig ML (1977) Structure of the semiquinone form of flavodoxin from *Clostridium MP*: extension of 1.8 Å resolution and some comparisons with the oxidized state. J Mol Biol 117:195–225.
17. Afonine PV, Grosse-Kunstleve RW, Echols N, Headd JJ, Moriarty NW, Mustyakimov M, Terwilliger TC, Urzhumtsev A, Zwart PH, Adams PD (2012) Towards automated crystallographic structure refinement with phenix.refine. Acta Crystallogr D Biol Crystallogr 68: 352–367.
18. Garman EF (2010) Radiation damage in macromolecular crystallography: what is it and why should we care? Acta Crystallogr D Biol Crystallogr 66:339–351.
19. Hersleth H-P, Andersson KK (2011) How different oxidation states of crystalline myoglobin are influenced by x-rays. Biochim Biophys Acta 1814:785–796.
20. Røhr ÅK, Hersleth H-P, Andersson KK (2010) Tracking flavin conformations in protein crystal structures with Raman spectroscopy and QM/MM calculations. Angew Chem Int Ed 49:2324–2327.
21. Hu Y, Li Y, Zhang X, Guo X, Xia B, Jin C (2006) Solution structures and backbone dynamics of a flavodoxin MioC from *Escherichia coli* in both apo- and holoforms: Implications for cofactor binding and electron transfer. J Biol Chem 281:35454–35466.

22. Ye Q, Hu Y, Jin C (2014) Conformational dynamics of *Escherichia coli* flavodoxins in apo- and holo-states by solution NMR spectroscopy. PLoS One 9:e103936.
23. Battye TGG, Kontogiannis L, Johnson O, Powell HR, Leslie AGW (2011) iMOSFLM: a new graphical interface for diffraction-image processing with MOSFLM. Acta Crystallogr D Biol Crystallogr 67:271–281.
24. Evans PR, Murshudov GN (2013) How good are my data and what is the resolution? Acta Crystallogr D Biol Crystallogr 69:1204–1214.
25. McCoy AJ, Grosse-Kunstleve RW, Adams PD, Winn MD, Storoni LC, Read RJ (2007) Phaser crystallographic software. J Appl Crystallogr 40:658–674.
26. Fantuzzi A, Artali R, Bombieri G, Marchini N, Meneghetti F, Gilardi G, Sadeghi SJ, Cavazzini D, Rossi GL (2009) Redox properties and crystal structures of a *Desulfovibrio vulgaris* flavodoxin mutant in the monomeric and homodimeric forms. Biochim Biophys Acta 1794:496–505.
27. Murshudov GN, Skubák P, Lebedev AA, Pannu NS, Steiner RA, Nicholls RA, Winn MD, Long F, Vagin AA (2011) REFMAC5 for the refinement of macromolecular crystal structures. Acta Crystallogr D Biol Crystallogr 67:355–367.
28. Adams PD, Afonine PV, Bunkoczi G, Chen VB, Davis IW, Echols N, Headd JJ, Hung L-W, Kapral GJ, Grosse-Kunstleve RW, McCoy AJ, Moriarty NW, Oeffner R, Read RJ, Richardson DC, Richardson JS, Terwilliger TC, Zwart PH (2010) PHENIX: a comprehensive Python-based system for macromolecular structure solution. Acta Crystallogr D Biol Crystallogr 66:213–221.
29. Chen VB, Arendall WB III, Headd JJ, Keedy DA, Immormino RM, Kapral GJ, Murray LW, Richardson JS, Richardson DC (2010) MolProbity: all-atom structure validation for macromolecular crystallography. Acta Crystallogr D Biol Crystallogr 66:12–21.
30. Emsley P, Lohkamp B, Scott WG, Cowtan K (2010) Features and development of Coot. Acta Crystallogr D Biol Crstallogr 66:486–501.
31. Schrodinger, LLC (2015) The PyMOL Molecular Graphics System, Version 1.8. New York: Schrodinger, LLC.
32. Zeldin OB, Gerstel M, Garman EF (2013) RADDOSE-3D: time- and space-resolved modelling of dose in macromolecular crystallography. J Appl Crystallogr 46: 1225–1230.
33. Zeldin OB, Brockhauser S, Bremridge J, Holton JM, Garman EF (2013) Predicting the X-ray lifetime of protein crystals. Proc Natl Acad Sci USA 110:20551.
34. Holm L, Rosenström P (2010) Dali server: conservation mapping in 3D. Nucleic Acids Res 38:W545–W549.
35. Waterhouse AM, Procter JB, Martin DMA, Clamp M, Barton GJ (2009) Jalview Version 2—a multiple sequence alignment editor and analysis workbench. Bioinformatics 25:1189–1191.
36. Livingstone CD, Barton GJ (1993) Protein sequence alignments: a strategy for the hierarchical analysis of residue conservation. Bioinformatics 9:745–756.